Ocean variability in Monterey Bay, California and connections to global climate, 1989-2016.

Gabriela Chavez, New York University

Mentor: Tim Pennington

Summer 2016

Keywords: El Niño, variability, principle component analysis, modes, anomalies

ABSTRACT

This study analyzes a 27-year time series dataset at a fixed location produced by 774 CTD casts in Monterey Bay. Primary component analysis (PCA) is used to reveal the dominant modes of variability in temperature, salinity, nitrate concentration, chlorophyll, and primary production. In physical and chemical parameters, the first mode is consistent with ENSO signatures and correlates highly with the Multivariate ENSO Index (MEI), the Pacific Decadal Oscillation (PDO), the El Niño Modoki index (EMI), and the North Pacific Gyre Oscillation (NPGO). The first mode of variability in the biological parameters does not appear to be linked directly to ENSO and does not correlate to the global climate indices either but is instead characterized by a punctuated increase in positive anomalies in the second half of the time series. Furthermore, the PCA reveals that the local effect of the most recent El Niño event, predicted to be extraordinary, and the warm "Blob" of 2014/15 were weak with respect to prior events in terms of their impact on Monterey Bay.

I. INTRODUCTION

The winter of 2015/16 saw the development of an El Niño event and the previous year saw the arrival of anomalously warm sea surface temperatures linked to unusual warming in the Northeastern Pacific termed "the Blob" (Bond et al., 2015). Globally, sea surface temperature anomalies have seen an upward trend in the last century with the last

year registering as the largest positive anomaly in a 130-year global dataset (updated records from Messié and Chavez, 2011; http://www.mbari.org/science/upper-ocean-systems/biological-oceanography/publication-global-modes-of-sea-surface-temperature/). Prior to the arrival of this El Niño, models and record-breaking measurements of sea surface temperature in the Western Pacific suggested that this event could be possibly the largest of its kind by the time it reached the Americas, earning it the nickname the "Godzilla El Niño' by fall of 2015. In California, however, the wintertime peak of this event proved to be less impactful than the last large El Niño of 1997/98. Most notably absent were the heavy rainfalls brought by the earlier event but recorded anomalies in other parameters were for the most part smaller and less persistent as well. Monterey Bay Aquarium Research Institute's shipboard CTD sampling effort of different sites in the Bay, the Monterey Bay Time Series (1989-present), presents an invaluable record of changing ocean parameters including but not limited to temperature, salinity, nutrient content, chlorophyll, and levels of primary production. This study set out to analyze different datasets produced by these cruises over the 27-year period, to see what trends could be discerned and what such a record could tell us about how oceanographic conditions are changing in Monterey Bay. This study also sought to examine the most recent years captured in the time series to elucidate the manifestation of the 2014/15 warm Blob and the 2015/16 El Niño and how these events compared to the El Niño of 1997/98 both locally and globally.

II. MATERIALS

a. Monterey Bay Time Series Datasets

A 27-year shipboard time series has been compiled by 774 unique cruises, during which several stations in Monterey Bay are occupied and sampled by MBARI ships. Although multiple moorings are occupied during each cruise, from near-shore (C1, 5.5km from Moss Landing), to the mouth of the bay (M1, 18.5km from Moss Landing), to off-shore (M2, 55.5km from Moss Landing), this study focused only on the datasets produced at M1. Temperature, salinity, nitrate, chlorophyll, and primary production were chosen as the parameters of interest as they represent physical, chemical, and biological properties of the bay. A CTD and 12-bottle Niskin rosette were used to collect

temperature and salinity data (CTD) and determine nitrate concentration, chlorophyll concentration, and primary production rates (Niskins).

b. Regional, Global Climate Indices and Equatorial Sea Surface Temperature indices

A suite of climate indices and oscillations were used for comparison to variability in the MBTS: the Multivariate ENSO Index (MEI), the Pacific Decadal Oscillation (PDO), the North Pacific Gyre Oscillation, (NPGO), and the El Niño Modoki Index (EMI). These indices were downloaded from the internet and originally sourced from Wolter and Timlin (1993), Mantua et al. (1997), DiLorenzo et al. (2008), and Ashok et al. (2007), respectively. Monthly SST anomalies for the Niño 1+2, 3, 3.4, and 4 quadrants of the Pacific from 1982 to the presents are calculated by NOAA and published online (http://www.cpc.ncep.noaa.gov/data/indices/sstoi.indices). These values were also used for comparison to local variability in Monterey Bay.

III. METHODS

a. Calculation of Anomalies and May-April Year Convention

In an attempt to stay as close as possible to raw data, anomalies were calculated without smoothing, normalization, or filtration. The raw data were placed into 14-day bins, an average year was calculated and then subtracted from the values to produce the anomalies.

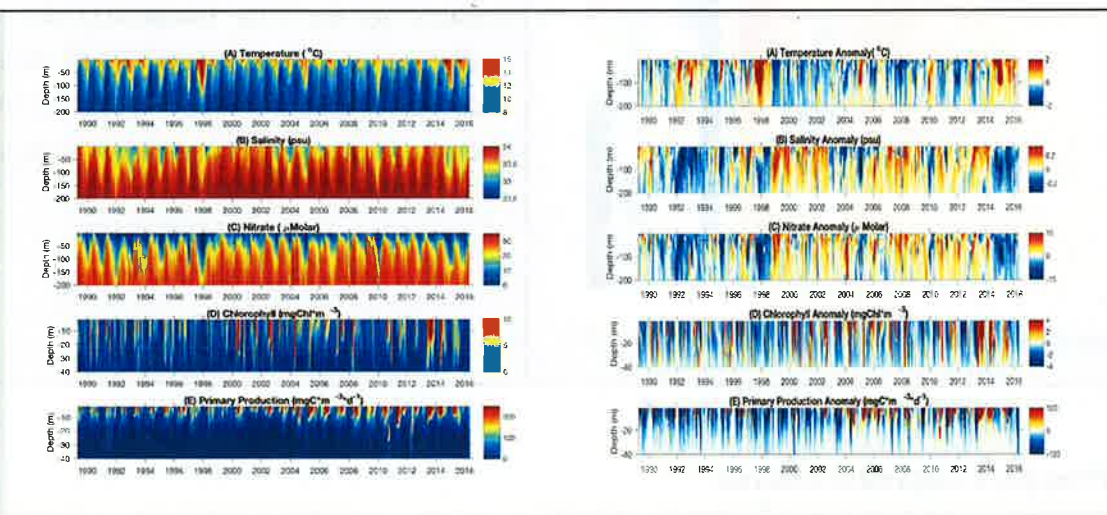

Figure 1. Raw data from 0-200 meters from April 1989- June 2016 and calculated anomalies for same time period and depths. Updated figures from Pennington and Chavez (submitted for publication, 2011).

Once calculated, the 14-day bins were arranged into 27 12-month sections beginning on May 1, 1989 and ending on April 30, 2016. The decision to begin the "year" on May 1 rather than January 1 allowed each El Niño event in the series to be captured as a whole in each section without splitting it between calendar years. Rather than centering spring and summer upwelling, the "El Niño Year" centers winter warming in every year of the time series, including years of interest such as 1997/98, 2014/15, and 2015/16 (Fig. 1)

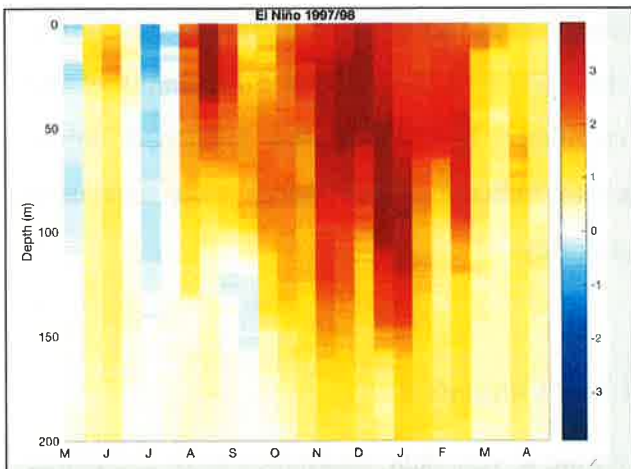

Figure 2a. Temperature anomaly section of 1997/98.

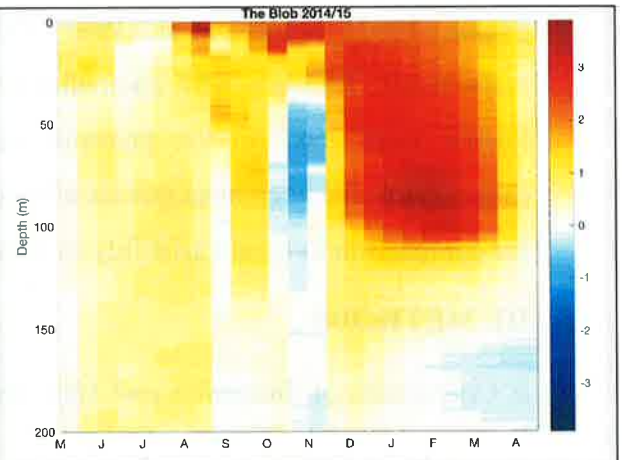

Figure 2b. Temperature anomaly section of 2014/15

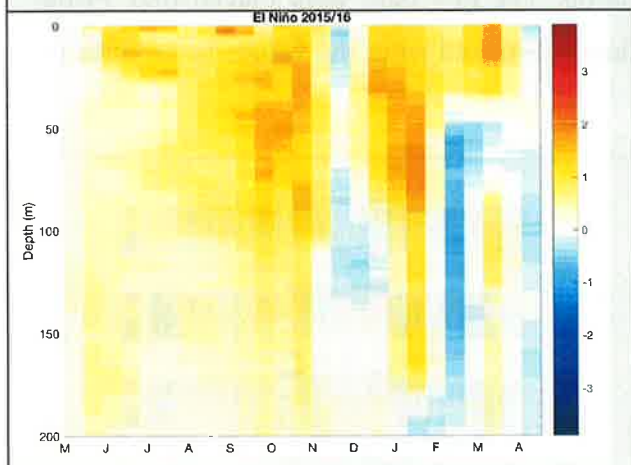

Figure 2c. Temperature anomaly section of 2015/16

Figure 2. Anomalies in all parameters were binned into 14-day bins and arranged into 12-month sections beginning in May and ending in April. For parameters measured by the CTD (temperature and salinity), anomalies to a depth of 200 meters were included. For bottle-derived data, anomalies to a depth of 100 meters or 0.1% light level (primary production) were included.

b. Principal Component Analysis

The application of principal component analysis (PCA), also known as empirical orthogonal functions (EOF), in this study was modeled after the treatment of SST

anomalies by Messié and Chavez (2011) but adapted to analyze anomalies temporally from the sea surface down through the water column at a single point (M1) rather than a single depth over a large geographic area. The 12-month anomaly sections for each of the five parameters were the primary inputs for the principal component analysis. The resulting modes are composed of a "spatial" (in reality, spatio-temporal) EOF— a fortnight by fortnight evolution of anomalies through the water column for a 12-month period starting in May and ending in April— and a temporal principal component (PC) that gives a single value for each year in the time series. The mode is determined by multiplying the pattern of anomalies in the EOF by the value of the PC (see Figure 2).

c. Correlations to Global Indices and SST anomalies for Niño 1+2, 3, 3.4, and 4

In order to correlate the resulting PC values for each of the five parameters (one value for each year) to the indices, the monthly values for each index and the monthly anomalies for each *Niño* region were averaged over yearlong periods (May to April) for each year of the time series. The resulting averages were then correlated to the PCs.

RESULTS

a. Temperature

i. EOF and PC

The first mode of the principle component analysis for temperature anomalies explains 46.5% of the variability in this parameter over the 27-year period. Subsequent modes account for 14% or less of variability and were not determined to be independent of Mode 1. The resulting PCs of subsequent modes failed to correlate with any of the indices. For these reasons, only Mode 1 was described and discussed in this study. The biggest loading of Mode 1 is the El Niño year of 1997/98 (PC=1). When the PC=1, the EOF displays a pattern that closely resembles the true spread of anomalies in 1997/98 (Figure1a). Nearly entirely positive anomalies throughout the whole year with anomalies >2˚C in the upper 50 meters developing in the fall months, reaching a maximum depth of ~150 meters in December and January (the peak of most El Niño events) and abating toward the surface once again in spring. The maximum anomalies (>3˚C) occur in

December and January at a depth of ~100 meters. This is consistent with El Niño-like deepening of the thermocline, which during normal conditions is between 60-80 meters at M1. Other known El Niños and El Niño Modokis (1992/93, 2004/05, 2009/10, 2015/16) are also positive values. The "Blob" (2014/15) is also much greater than 0, greater even than 2015/16 although we know that this phenomena was not linked to ENSO dynamics. In years when the PC is less than 0, the anomalies are inverted and become negative (La Niña). The greatest negative year in the PC is 2007/08.

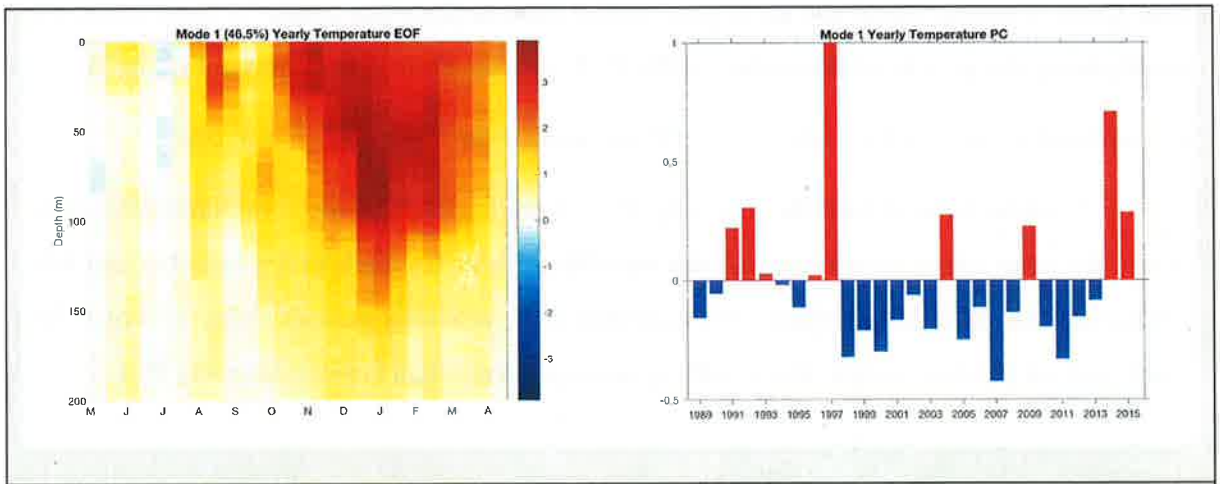

Figure 3. On the left is the EOF of Mode 1 for temperature anomalies and on the right is the principle component (PC). Together they depict the evolution of El Niño-like anomalies through the water column over the course of an individual year and over the course of the time series.

ii. Correlation to indices

Once the indices were averaged to produce a single annual value, the temperature PC was found to correlate to the MEI, PDO, Niño 1+2, 3, 3.4, 4* at the $p<.01$ level (*$p<.05$). When the MEI and PC are plotted together, El Niño (2015/16) and the Blob (2014/15) prove to be outliers although El Niño 1997/98 provides both the largest x and y values.

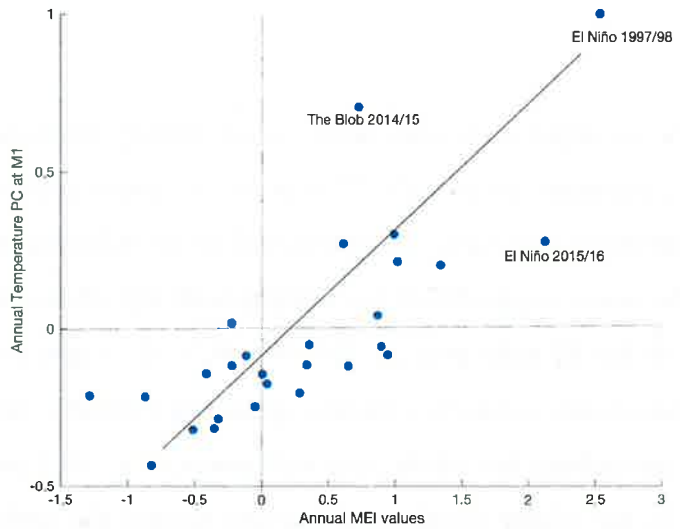

Figure 4. A scatterplot of the average MEI values for each year of the time series and the PC values. Each dot represents one year with El Niño 1997/98, The Blob 2014/15, and El Niño 2015/16 highlighted. There was a strong correlation (r=0.78) with 2014/15 and 2015/16 standing as noticeable outliers.

When correlated with Niño 4, however, the plot reveals that El Niño 2015/16 was in fact warmer than 1997/98 and 2014/15 in that region of the Pacific. Still, it does not differ greatly from the trend line.

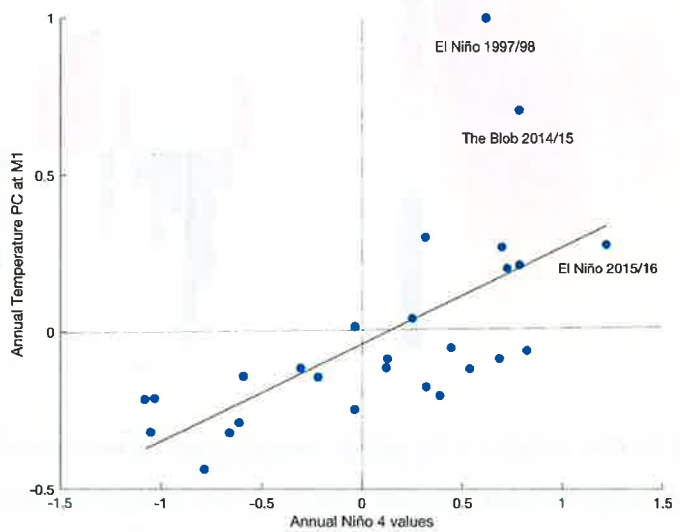

Figure 5. A scatterplot of the average Niño 4 values for each year of the time series and the PC values. El Niño 1997/98, The Blob 2014/15, and El Niño 2015/16 are highlighted. There was a strong correlation (r=0.64).Unlike in Monterey Bay, 2015/16 had a greater effect than either 2014/15 or 1997/98.

b. Salinity

The first mode of the principle component analysis for salinity anomalies explains 38.4% of the variability in this parameter over the 27-year period. Subsequent modes account for 14.8% or less of variability and were not determined to be independent of Mode 1. The resulting PCs of subsequent modes failed to correlate with any of the indices. The biggest loading of Mode 1 is the El Niño year of 1992/93 (PC=-1). When the PC=-1, the EOF displays a pattern that closely resembles the true spread of anomalies in 1992/93. Entirely positive anomalies throughout the whole year with anomalies <-0.3 psu between 50-150 meters developing in the winter months and moving toward the surface in spring. The maximum anomalies (<-0.5 psu) occur near the surface in March and April. This is consistent with El Niño-like freshening. The salinity develops later than the temperature signal. Other known El Niños and El Niño Modokis (1997/98, 2004/05, 2009/10, 2015/16) are also negative values. The "Blob" (2014/15) is also much less than 0. In years when the PC is greater than 0, the anomalies are inverted and become positive (saltier). The greatest positive year in the PC is 1998/99.

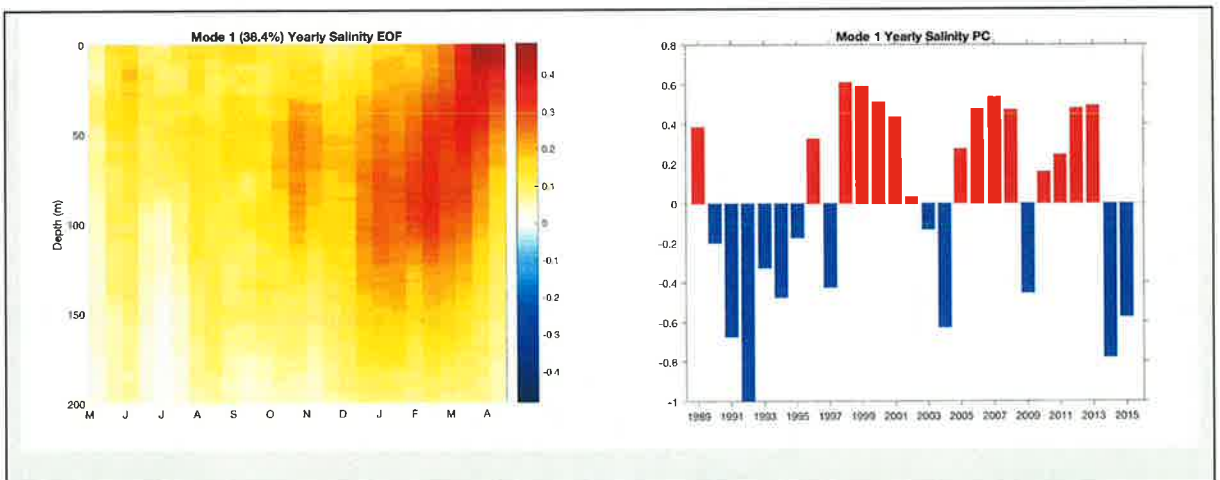

Figure 6. On the left is the EOF of Mode 1 for salinity anomalies and on the right is the principle component (PC). Together they depict the evolution of El Niño-like anomalies through the water column over the course of a year (EOF) and over the course of the time series (PC). The salinity signature comes later in the year than temperature. This might mean that first, the depression of the thermocline occurs as a result of Kelvin waves and that this then allows for the toward-shore movement of the fresher California Current.

ii. Correlation to indices

Once averaged to produce a single annual value, the salinity PC was found to correlate to the MEI, PDO, NPGO, EMI, and Niño 1+2*, 3, 3.4, 4 at the p<.01 level (*p<.05). When the MEI and the PC are plotted together, neither El Niño (2015/16) nor the Blob (2014/15) show up as distinct outliers.

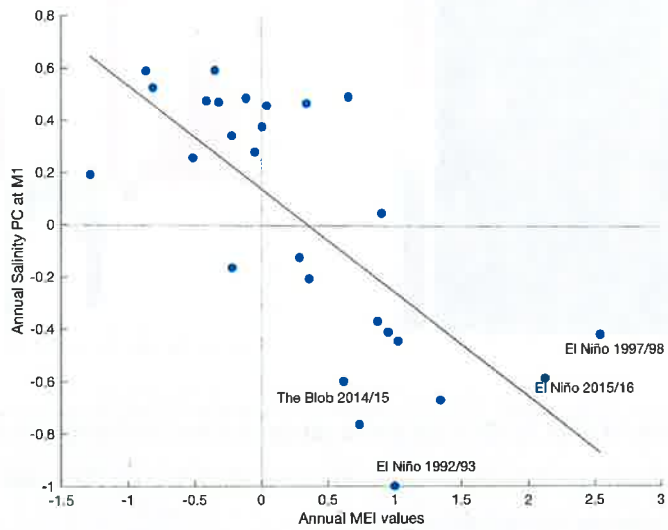

Figure 7. A scatterplot of the average MEI values for each year of the time series and the PC values. Each dot represents one year with El Niño 1997/98, The Blob 2014/15, and El Niño 2015/16 highlighted as well as El Niño 1992/93, the biggest loading for the mode. Unlike temperature, 2014/15 and 2015/16 registered as bigger events than 1997/98.

c. Nitrate

The first mode of the principle component analysis for nitrate anomalies explains 27.4% of the variability in this parameter over the 27-year period. Subsequent modes account for 14% or less of variability and were not determined to be independent of Mode 1. The resulting PCs of subsequent modes failed to correlate with any of the indices. The biggest loading of Mode 1 is the El Niño year of 1997/98 (PC=1). When the PC=1, the EOF displays a pattern that closely resembles the true spread of anomalies in 1997/98. Nearly entirely negative anomalies throughout the whole year with anomalies <-5μ Molar

between 20-100 meters developing in the fall months. Between January and April anomalies of <-8μ Molar occur in the range 20-100 meters. This is consistent with El Niño-like deepening of the thermocline (nutricline). Other known El Niños and El Niño Modokis (1992/93, 2004/05, 2009/10, 2015/16) are also positive values. The "Blob" (2014/15) is also much greater than 0. In years when the PC is less than 0, the anomalies are inverted and become positive. The greatest negative year in the PC is 2003/04.

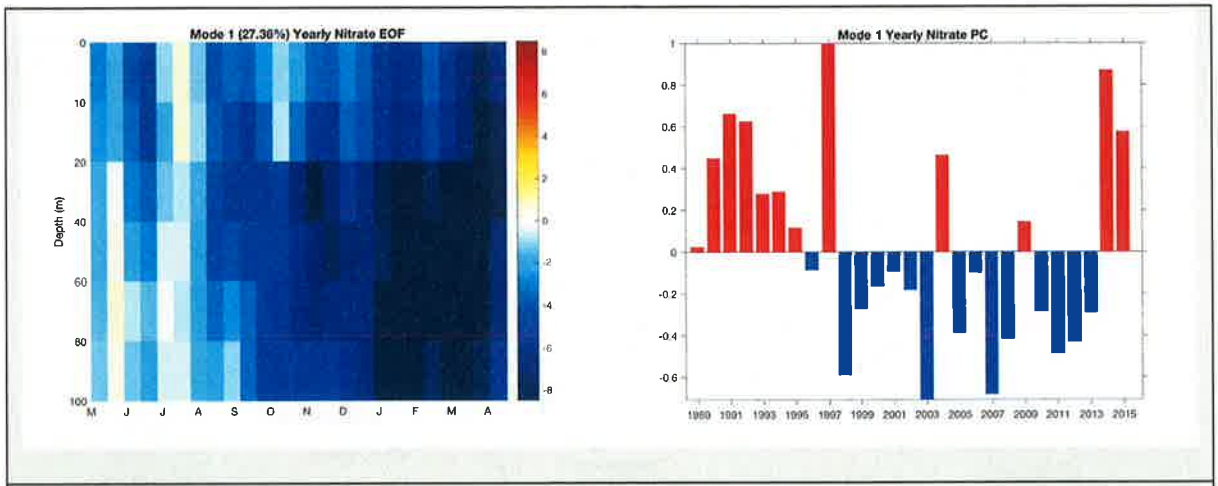

Figure 8. On the left is the EOF of Mode 1 for nitrate anomalies and on the right is the principle component (PC). Together they depict the evolution of El Niño-like anomalies through the water column over the course of a individual year and over the course of the time series.

ii. Correlation to indices

Once averaged to produce a single annual value, the nitrate PC was found to correlate to the MEI, PDO, NPGO, EMI, and Niño 1+2, 3, 3.4, 4 at the $p<.01$ level. When the MEI and the PC are plotted together, the scatterplot resembles that of temperature although there is greater spread in prior years of the time series and El Niño (2015/16) lies closer to the trend line than the Blob (2014/15)

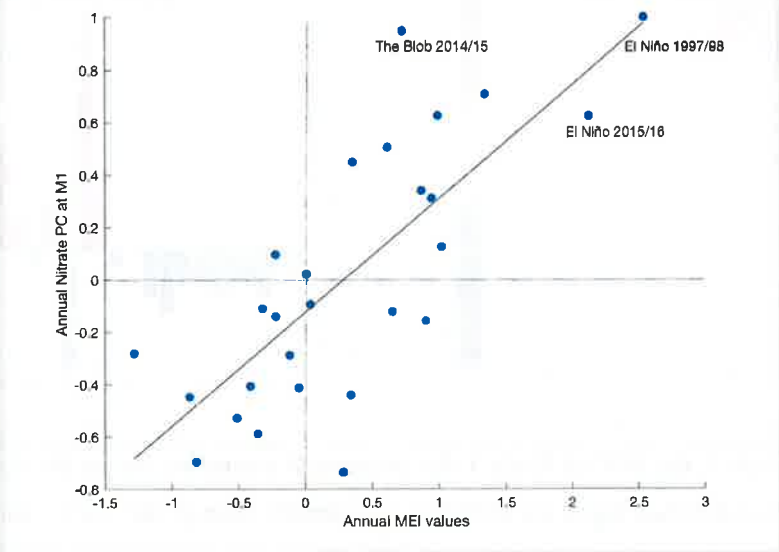

Figure 9. A scatterplot of the average MEI values for each year of the time series and the PC values. Each dot represents one year with El Niño 1997/98, The Blob 2014/15, and El Niño 2015/16 highlighted. The pattern is very similar to that of temperature, although 2015/16 lies closer to the trend line.

d. Chlorophyll

The first mode of the principle component analysis for chlorophyll anomalies explains 23.6% of the variability in this parameter over the 27-year period. Subsequent modes account for 15% or less of variability and were not determined to be independent of Mode 1. The biggest loading of Mode 1 is the El Niño year of 2002/03 (PC=1). When the PC=1, the EOF displays positive surface anomalies in August and September, with a maximum of >10mgChl/m^3. In general the PC can be characterized as having mostly negative values until 2000 with mostly positive values after that.

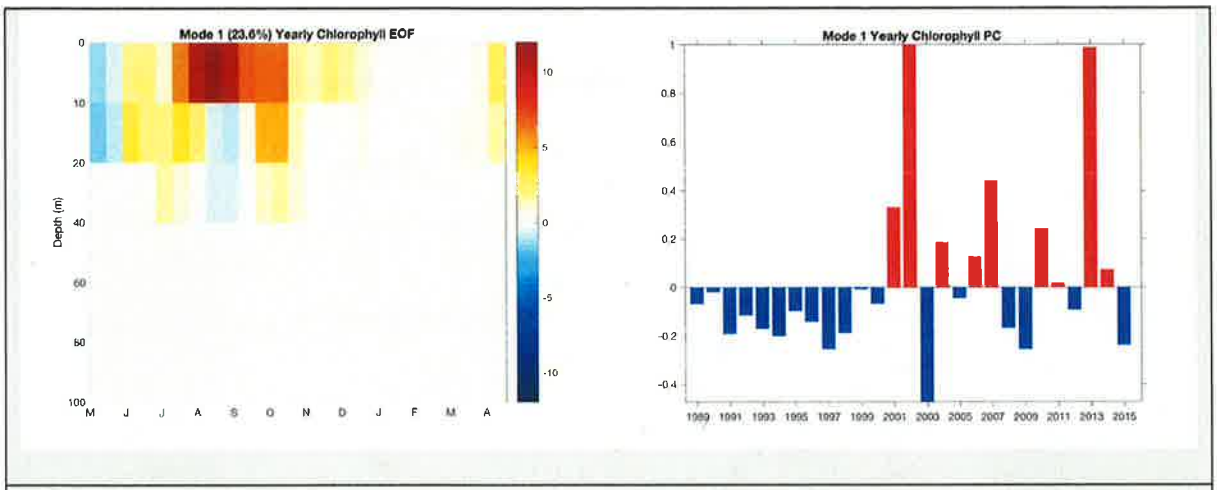

Figure 10. On the left is the EOF of Mode 1 for chlorophyll anomalies and on the right is the principle component (PC). Together they depict the evolution of anomalies through the water column over the course of an individual year and over the course of the time series.

ii. Correlation to indices

Once averaged to produce a single annual value, the chlorophyll PC was not found to correlate to the MEI, PDO, NPGO, EMI, or Niño 1+2*, 3, 3.4, 4. When the MEI and the PC are plotted together, the two years where the PC was at or near 1 (2002/03 and 2013/14) are clear outliers. Excluding these values gives a significant ($p<.05$) correlation to the MEI ($r=0.47$).

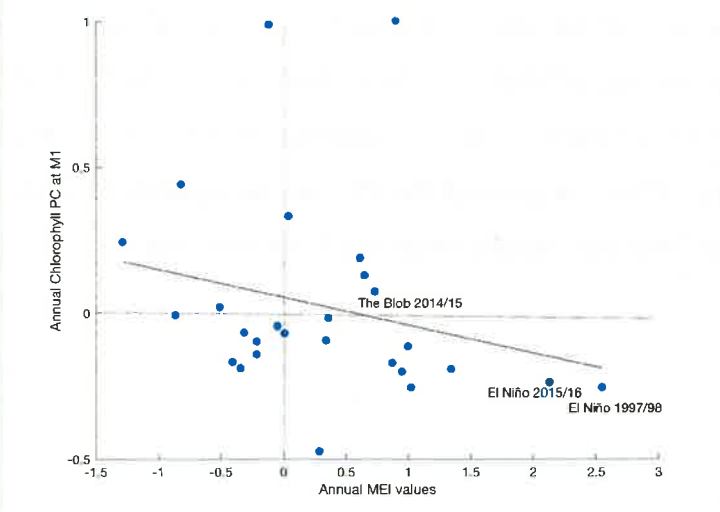

Figure 11. A scatterplot of the average MEI values for each year of the time series and the PC values. Each dot represents one year with El Niño 1997/98, The Blob 2014/15, and El Niño 2015/16 highlighted. Interestingly, a general trend is discernible with 2 distinct outliers (2002/03 and 2013/14).

e. Primary Production

The first mode of the principle component analysis for primary production anomalies explains 37.1% of the variability in this parameter over the 27-year period. Subsequent modes account for 22% or less of variability and were not determined to be independent of Mode 1. The biggest loading of Mode 1 is 2013/14. When the PC=1, the EOF displays a pattern of positive anomalies from May to August, reaching a maximum of >800mgC/m^3/day in the 100% light level in June. There is an obvious upward trend in the PC with the value switching phase from negative to positive in 2004.

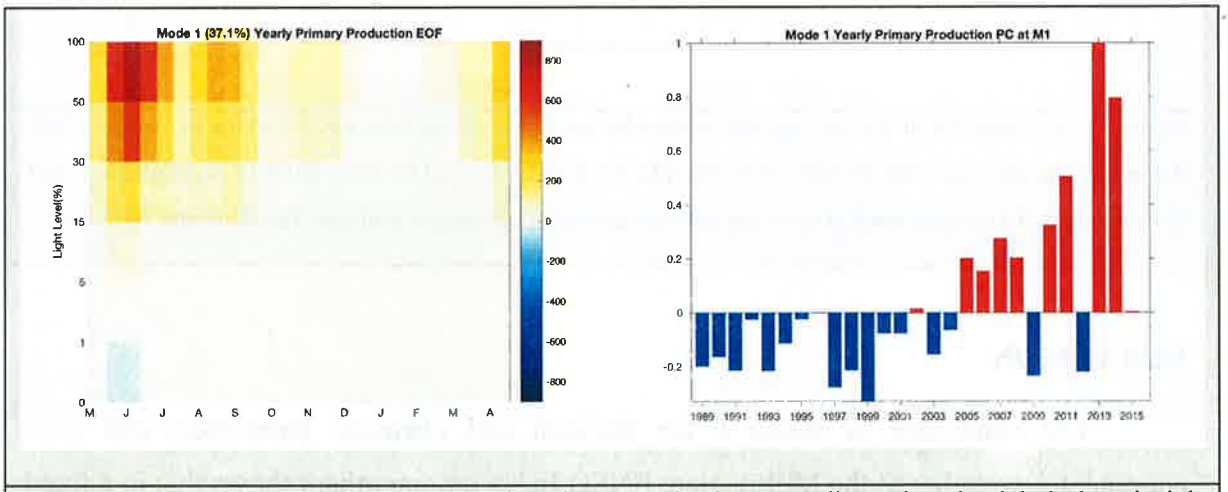

Figure 12. On the left is the EOF of Mode 1 for primary production anomalies and on the right is the principle component (PC). Together they depict the evolution of anomalies through the water column over the course of an individual year and over the course of the time series.

ii. Correlation to indices

Once averaged to produce a single annual value, the primary production PC was not found to correlate to the MEI, PDO, NPGO, EMI, or Niño 1+2*, 3, 3.4, 4 When the MEI and the PC are plotted together, the Blob (2014/15) and 2013/14 (PC=1) show up as distinct outliers. Excluding these values gives a significant ($p<.05$) correlation to the MEI ($r=0.43$).

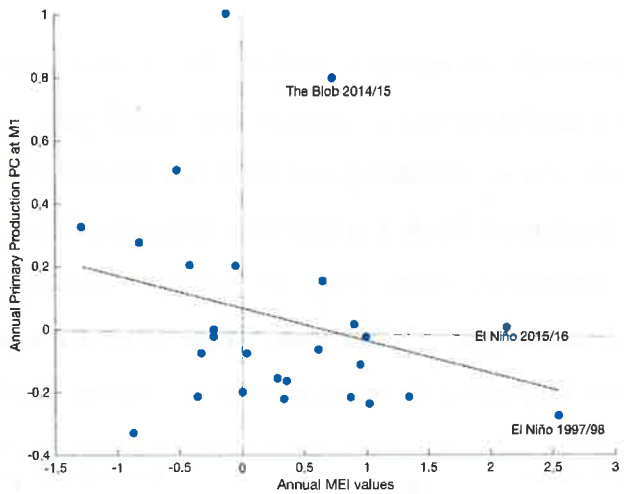

Figure 13. A scatterplot of the average MEI values for each year of the time series and the PC values. Each dot represents one year with El Niño 1997/98, The Blob 2014/15, and El Niño 2015/16 highlighted. Much like chlorophyll a general trend is apparent with the except of two major outliers (The Blob and 2013/14).

DISCUSSION

The coherence of Mode 1 for physical and chemical parameters and their consistent correlation to the Multivariate ENSO Index among others shows that in a fixed location time series only 27-years-old, the impact of El Niño is similarly apparent to the impact it has had globally over more than a century. The first mode of global SST variability found by Messié and Chavez (2011) also reveals a classical El Niño pattern and a PC that correlates to the MEI.

Contrary to predictions, however, the El Niño of 2015/16 did not have nearly as big of an impact locally as the 1997/98 event and registered as less anomalous than even the previous year in regard to nearly all parameters studied (the magnitude of the PC in Mode 1 of chlorophyll anomalies was greater than 2014/15 but was opposite in sign). Jacox et al. (2016) had similar findings when comparing the impacts of the El Niño 2015/16 to those of 1997/98 and 1982/83 in the California Current system, stating that "while positive SST anomalies were also observed near shore during the 2015-16 El Niño…cross-shore gradients were much less pronounced and the broad-scale temperature

structure appears to be more consistent with ongoing decay of pre-existing northeast Pacific warm anomalies [Bond et al., 2015; Zaba and Rudnick, 2016] than with the warming signature of El Niño." However, both that study and this one show that when classifying an El Niño, the impacts from region to region do not necessarily correspond. While the eastern Pacific saw an event much smaller than the large events of the past, the western Pacific (Niño 3.4 and 4) did see its warmest ever El Niño in 2015/16.

The lack of correlation between the biological parameters and ENSO is noteworthy. The EOFs and PCs for both chlorophyll and primary production depict a pattern of anomalies that develops each year in either the early fall (chlorophyll) or spring (primary production). Because these seasons lay outside of El Niño's greatest influence, it is understandable that the biological dynamics over the years cannot be seen to be affected by these oscillations, at least in the time period available for study. It could well be that as the time series continues, a correlation would become apparent with a lower frequency oscillation like the PDO. Another consideration is a possible calculation error. The distinct increase in both these variables in the latter half of the time series cannot be easily explained by environmental factors and when the two largest outliers are removed from both datasets, a significant though still small correlation between the PCs and the MEI is revealed.

CONCLUSIONS and RECOMMENDATIONS

Principle component analysis of anomalies in temperature, salinity, nitrate, chlorophyll, and primary production through the water column in a 27-year fixed location CTD time series reveals a mode of variability highly correlated to ENSO in physical and chemical parameters and a mode independent of ENSO in biological parameters. Furthermore, the El Niño of 2015/16 is shown to have had much less impact in Monterey Bay than the El Niño of 1997/98, despite predictions that it would be remarkable. In biological parameters, no correlation with any of the indices considered was found. Instead, the PCs for both chlorophyll and primary production were characterized by a punctuated increase in positive anomalies in the second half of the time series. For greater

understanding and in an attempt to minimize the effect of possible error, it is recommended that the same analysis be carried out for both the C1 and M2 stations as well as updated regularly as the time series continues.

ACKNOWLEDGEMENTS

This project would not have been possible without a team of support. My mentor Tim Pennington guided me through both the theoretical aspects of the study and the tangible process of collecting the data I was studying by bring me along on this summer's MBTS cruises. He showed me how much hard work and dedication it takes to realize a long-term sampling effort of this magnitude. Reiko Michisaki was infinitely patient with me as I learned a new language I had never before spoken: MatLab. I would have been lost without her. Monique Messié's previous studies and expertise in data processing provided me with inspiration and clarity throughout this endeavor. Francisco Chavez made time for endless consultation and gave me a better understanding of the larger oceanographic dynamics that framed this paper. George Matsumoto and Linda Kuhnz integrated the entire intern group seamlessly into the MBARI community and made this one of the most pleasant work environments I have ever known. Alaina Smith and Bryce Corbett provided emotional support throughout the entire summer. Thank you all.

REFERENCES

Ashok, Karumuri, Swadhin K. Behera, Suryachandra A. Rao, Hengyi Weng, and Toshio Yamagata. "El Niño Modoki and its possible teleconnection." *Journal of Geophysical Research* (2007).

Bond, Nicholas A., Meghan F. Cronin, Howard Freeland, and Nathan Mantua. "Causes and impacts of the 2014 warm anomaly in the NE Pacific." *Geophysical Research Letters* (2015). Web.

Di Lorenzo E., Schneider N., Cobb K. M., Chhak, K, Franks P. J. S., Miller A. J., McWilliams J. C., Bograd S. J., Arango H., Curchister E., Powell T. M. and P. Rivere. "North Pacific Gyre Oscillation links ocean climate and ecosystem change." *Geophysical Research Letters* (2008). Web.

Jacox, Michael G., Elliott L. Hazen, Katherine D. Zaba, Daniel L. Rudnick, Christopher A. Edwards, Andrew M. Moore, and Steven J. Bograd. "Impacts of the 2015-2016 El Niño on the California Current System: Early Assessment and Comparison to past Events." *Geophysical Research Letters* (2016). Web.

Mantua, N.J. and S.R. Hare, Y. Zhang, J.M. Wallace, and R.C. Francis. "A Pacific interdecadal climate oscillation with impacts on salmon production." Bulletin of the American Meteorological Society (1997).

Messié, Monique and Francisco Chavez. "Global Modes of Sea Surface Temperature Variability in Relation to Regional Climate Indices." *Journal of Climate* (2016). Web.

Pennington, Tim and Francisco Chavez. "Decadal-scale oceanographic fluctuations in Monterey Bay, California, 1989-2011." Deep-Sea Research (in revision).

Wolter, K., and M.S. Timlin. "Monitoring ENSO in COADS with a seasonally adjusted principal component index" *Proc. of the 17th Climate Diagnostics Workshop (1993). Web.*

APPENDIX

	MEI	NPGO	PDO	EMI
Temperature	**0.78**	-0.40	**0.71**	0.31
Salinity	**-0.71**	**0.61**	**-0.68**	**-0.62**
Nitrate	**-0.76**	**0.56**	**-0.65**	**-0.51**
Chlorophyll	0.24	-0.24	0.13	-0.10
Primary Prod	0.28	0.05	0.06	0.04

	EN 1+2	EN 3	EN 3.4	EN 4
Temperature	**0.75**	**0.79**	**0.75**	**0.64**
Salinity	-0.45	**-0.61**	**-0.68**	**-0.69**
Nitrate	**-0.59**	**-0.69**	**-0.72**	**-0.67**
Chlorophyll	0.37	0.25	0.15	0.03
Primary Prod	0.19	0.20	0.19	0.08

Table 1. Correlations between eight different climate indices and the PCs for each of the five parameters studied. Bold values have a p-value <.01.